

Dynamics of a headwater system and peatland under current conditions and with climate change

Journal:	<i>Hydrological Processes</i>
Manuscript ID:	HYP-12-0676.R1
Wiley - Manuscript type:	Research Article
Date Submitted by the Author:	n/a
Complete List of Authors:	Levison, Jana; Guelph University, School of Engineering Larocque, Marie; University of Quebec at Montreal, Earth and atmospheric Sciences Véronique, Fournier; Université du Québec à Montréal, Sciences de la Terre et de l'atmosphère Gagné, Sylvain; Université du Québec à Montréal, Sciences de la Terre et de l'atmosphère Pellerin, Stéphanie; Université de Montréal, Biologie Ouellet, Marie-Audray; Université du Québec à Montréal, Sciences de la Terre et de l'atmosphère
Keywords:	Peatland, Headwater system, Climate change, Groundwater flow modeling, Covey Hill (Quebec, Canada)

SCHOLARONE™
Manuscripts

Review

1
2
3 1
4
5 2
6
7 3
8
9 4
10
11
12 **DYNAMICS OF A HEADWATER SYSTEM AND PEATLAND UNDER CURRENT**
13
14 **CONDITIONS AND WITH CLIMATE CHANGE**
15
16
17
18
19
20
21
22

23 **J. Levison^{1,3}, M. Larocque^{1*}, V. Fournier¹, S. Gagné¹, S. Pellerin² and M.A. Ouellet¹**
24
25
26
27
28

29 13 ¹ Centre de recherche pour l'étude et la simulation du climat à l'échelle régionale, Département
30 des sciences de la Terre et de l'atmosphère – Université du Québec à Montréal, C.P. 8888, succ.
31 Centre-Ville, Montréal (QC), Canada ; tel : 514-987-3000 ext. 1515 ; fax : 514-987-7749;
32 larocque.marie@uqam.ca
33
34
35
36

37 17 ² Institut de recherche en biologie végétale, Université de Montréal, Jardin botanique de
38 Montréal, 4101 rue Sherbrooke est, H1X 2B2, Montréal, Québec, Canada;
39 stephanie.pellerin.1@umontreal.ca
40
41
42
43

44 20 ³ Current address: School of Engineering, University of Guelph, Richards Building, N1G 2W1,
45 Guelph, Ontario, Canada, jlevison@uoguelph.ca,
46
47
48

49 22 * Corresponding author
50
51
52
53
54
55
56
57
58
59
60

1
2
3 25 **ABSTRACT**
4

5 26 Interactions between headwater aquifers and peatlands have received limited scientific attention.
6
7 27 Hydrological stresses, including those related to climate change, may adversely impact these
8
9 28 interactions. In this study, the dynamics of a southern Quebec headwater system where a peatland
10
11 29 is present is simulated under current conditions and with climate change. The model is calibrated
12
13 30 in steady-state on field-measured data and provides satisfactory results for transient state
14
15 31 conditions. Under current conditions, simulations confirm that the peatland is fed by the fractured
16
17 32 bedrock aquifer year round and provides continuous baseflow to its outlets. Climate change is
18
19 33 simulated through its impact on groundwater recharge. Predicted precipitation and temperature
20
21 34 data from a suite of Regional Climate Model scenarios provide a net precipitation variation range
22
23 35 from +10% to -30% for the 2041-2070 horizon. Calibrated recharge is modified within this range
24
25 36 to perform a sensitivity analysis of the headwater model to recharge variations (+10%, -15% and
26
27 37 -30%). Total contribution from the aquifer to rivers and streams varies from +14% to -44% of the
28
29 38 baseline for +10% to -30% recharge changes from spring 2010 data, for example. With higher
30
31 39 recharge, the peatland receives more groundwater, which could significantly change its
32
33 40 vegetation pattern and eventually ecosystem functions. For -30% recharge, the peatland becomes
34
35 41 perched above the aquifer during the summer, fall and winter. Recharge reductions also induce
36
37 42 sharp declines in groundwater levels and drying streams.
38
39
40
41
42
43

44 **KEYWORDS**

45 Peatland; headwater system; climate change; groundwater flow modeling; Covey Hill; southern
46 Quebec Canada

47
48
49
50
51
52
53
54
55
56
57
58
59
60

1. INTRODUCTION

In Canada, peatlands cover up to 14% of the land area and comprise over 90% of present wetlands (Waddington et al., 2009). They are the most prevalent wetland type in the southern part of the province of Quebec (Ducks Unlimited Canada, 2006). Peatlands play an important ecological role in maintaining fragile habitats (e.g. Calmé et al., 2002). They contribute uniquely to both physical and chemical hydrologic processes including streamflow, evapotranspiration and water storage (Waddington et al., 2009). In eastern Canada, as in other parts of the world, peatlands are under threat from human activities, particularly urban expansion and agriculture (Poulin et al., 2004), and potentially climate change (Moore, 2002; Tarnocai, 2006). In general, very little is known about peatland hydrological dynamics and linkages to local or regional groundwater flow systems. This is especially true for headwater peatlands which can be significant hydrological reservoirs in environments where bedrock hydraulic conductivity is low and surrounding soils can be thin or nonexistent (Winter, 2000).

Numerical modeling of groundwater flow through the peat and in the adjacent aquifer can be used to better understand peatland-aquifer flow dynamics (Ackerman et al., 2009; Baird et al., 2011). In regional scale groundwater flow models, surface water features such as lakes and peatlands are typically represented using constant heads. This boundary condition overly constrains groundwater flow around the peatland and prevents any consideration of temporal variations of peatland-aquifer exchanges. For some peatland-specific studies, modeling simplifications such as two-dimensional representations and steady-state flow regimes (Lapen et al., 2005) limit the results about regional scale and seasonal hydrological processes. The modeling work of Reeve et al. (2001) is a notable exception to the constant head peatland representation or peatland-specific modeling simplifications. Using a regional groundwater flow model and an explicit representation of flow processes between the peatlands and the aquifer, they showed that in the lowland Lake Agassiz area, groundwater flow within the peatlands is driven by local flow systems.

1
2
3 74 Nevertheless, the scientific literature holds few such examples of regional scale peatland-
4
5 75 groundwater interaction models. Simulating groundwater flow in fractured bedrock aquifers itself
6
7 76 is challenging because of the heterogeneous distribution of conductive fractures (Cook, 2003).
8
9
10 77 This can be further complicated by large vertical gradients present in fractured bedrock headwater
11
12 78 basins. Using an explicit representation of a peatland in a model to accurately simulate transient
13
14 79 fractured bedrock aquifer-peatland interactions in a complex headwater context has not, to our
15
16 80 knowledge, been previously investigated.

17
18
19 81
20
21 82 Climate change impacts on groundwater resources at a regional scale are increasingly studied
22
23 83 (e.g. Jyrkama and Sykes, 2007; Scibek et al., 2007). Results from these studies in different
24
25 84 locations show the possibility of increases and decreases in groundwater recharge, depending on
26
27 85 the topography, geology and climate, leading to a variety of trends in groundwater levels. It is
28
29 86 recognized that headwater streams in small catchments are more likely to be vulnerable to low-
30
31 87 flow impacts than larger river systems (Winter, 2007). In headwater catchments with shallow
32
33 88 bedrock aquifers, groundwater is probably also highly vulnerable to climate variations because of
34
35 89 slopes and limited (or no) surficial material overlying formations with low permeability which
36
37 90 leads to greater runoff and less infiltration (Kosugi et al., 2006). Investigations of climate change
38
39 91 effects on peatlands have focused on peat interactions with the atmosphere, notably carbon
40
41 92 exchanges (Strack et al., 2004; Belyea and Malmer, 2004), and on hydrologic processes occurring
42
43 93 within the organic deposits (e.g. Whittington and Price, 2006). Recently the impact of climate
44
45 94 change on wetland interaction with the surrounding aquifer has been studied (e.g. Ackerman et
46
47 95 al., 2009; Herrera-Pantoja et al., 2011), finding in particular a vulnerability with declining
48
49 96 groundwater levels. Changes in peatland-aquifer connectivity can impact stream and wetland
50
51 97 biogeochemistry (Devito, 1995; Brassard et al., 2000) which can induce vegetation changes (e.g.
52
53 98 Salinas et al., 2000) and lead to a flashier response to rainfall events (Greyson et al., 2010).
54
55
56
57 99 However, the amount of hydrological change a headwater system and its ecosystem can sustain
58
59
60

1
2
3 100 before adverse impacts are observed is not well understood. In particular, the function of
4
5 101 peatlands in the hydrological and ecosystem resilience of headwater systems is mostly unknown.
6
7 102 This lack of knowledge limits the development and application of adaptation strategies such as
8
9 103 land and water resources management (e.g. protecting peatlands, reducing groundwater
10
11 104 withdrawal, and limiting deforestation and urban development) in headwater systems where
12
13 105 peatlands are present.
14
15
16 106

17
18 107 This research was initiated at the request of Nature Conservancy of Canada to better understand
19
20 108 the hydrological function of a headwater peatland recently identified for conservation. The goal
21
22 109 of this long term study is to determine if the peatland plays a role in maintaining groundwater
23
24 110 levels, as well as river baseflows, streams and springs which form habitats for endangered
25
26 111 salamander species (Larocque et al., 2006). Climate change was identified as the most eminent
27
28 112 threat to the low development Covey Hill area where the targeted headwater peatland is located.
29
30 113 This paper addresses these questions by using a numerical groundwater flow model to simulate
31
32 114 the dynamics of the headwater system under current conditions and with climate change-induced
33
34 115 recharge variations. Specifically, a groundwater flow model developed in MODFLOW
35
36 116 (Harbaugh, 2005) is used to simulate regional flows for the headwater system as well as local
37
38 117 aquifer-peatland interactions under current conditions and with a range of recharge scenarios
39
40 118 derived from Regional Climate Models.
41
42
43
44 119

45 46 47 120 **2. Study area**

48
49 121 The Covey Hill peatland is located within the Covey Hill Natural Laboratory (Larocque et al.,
50
51 122 2006), 74°00'W, 45°00'N, near the Canada-USA border in the Chateaugay River watershed
52
53 123 (Figure 1). Covey Hill is the most northward extension of the Adirondack Mountains. The highest
54
55 124 point on the hill is located 345 m above sea level. Covey Hill comprises Cambrian sandstone of
56
57 125 the Potsdam Group (Covey Hill Formation), deformed and fractured during the Appalachian
58
59
60

1
2
3 126 orogeny (Globensky, 1986). Groundwater flows in the fractured sandstone. This bedrock aquifer
4
5 127 is used by local residents for potable water supply.
6
7 128
8
9
10 129 The absence of surface deposits on large areas near the hilltop and south of the international
11
12 130 border shows the importance of erosion during the last ice advance (12 ky). In other areas, the hill
13
14 131 is covered by the thin, permeable and sandy Saint-Jacques till (Lasalle, 1981). Glaciolacustrine
15
16 132 sediments are found locally below 220 m above sea level (masl) (Parent and Occhietti, 1988).
17
18 133 Sandy beach deposits are located at the foot of the hill, between 80 and 100 masl (Tremblay et al.,
19
20 134 2010). Littoral sediments from the erosion of the rock substrate by the Champlain Sea and till are
21
22 135 abundant at the base of Covey Hill (see cross-section, Figure 1b). These sediments, composed of
23
24 136 highly permeable sands and gravels, are mostly located on the northern side of the hill. The
25
26 137 sandstone aquifer is generally unconfined over the study area. The till, silt and clay sediments in
27
28 138 the north are less permeable than the sandy deposits at the base of the hill. Groundwater flow
29
30 139 through the sandstone aquifer occurs in laterally-extensive sub-horizontal bedding planes,
31
32 140 connected by sub-vertical fractures and joints (Nastev et al., 2008). Covey Hill is considered an
33
34 141 important recharge area for the 2500 km² Chateauguay aquifer (Croteau et al., 2010). Near the
35
36 142 end of the last glaciation, the breakout of paleo-lake Iroquois through an outlet near Covey Hill
37
38 143 created a relatively impervious sandstone pavement (also called Flat Rock) that extends from
39
40 144 below the peatland approximately 30 km southeastward into the Champlain Valley in the United
41
42 145 States (Franzi et al., 2002). The Blueberry and Gouffre lakes are remnants of this catastrophic
43
44 146 event and form deep reservoirs which store significant volumes of water along the Allen River
45
46 147 (Barrington et al., 1992).
47
48 148
49
50
51
52
53 149 The Covey Hill peatland is one of the few remaining undisturbed peatlands in southern Quebec
54
55 150 and one of the oldest known in the province. Basal peat ¹⁴C dating shows that organic matter
56
57 151 started accumulating 13 250 years B.P., probably soon after the breakout of paleo-lake Iroquois
58
59
60

1
2
3 152 (Pellerin et al., 2007). The peatland covers an area of approximately 0.51 km² near the hilltop.
4
5 153 The peat averages 1.4 m deep and reaches 3.2 m in some areas (Rosa et al., 2008; see Figure 1b).
6
7 154 To the west, the peatland feeds the Outardes River and to the east it discharges in the Allen River.
8
9 155 Fournier (2008) used hydraulic gradients and a water budget to demonstrate that groundwater
10
11 156 flows year round from the surrounding bedrock aquifer into the peatland. A vegetation study also
12
13 157 identified a minerotrophic transition zone (lagg) between the forests located on the bedrock and
14
15 158 the central peatland ombrotrophic sector (Pellerin et al. 2009). Surface water input to the
16
17 159 peatland from runoff has not been observed since the start of the peatland monitoring and is
18
19 160 considered negligible. Based on the piezometric map of Covey Hill the area contributing
20
21 161 groundwater to the peatland is estimated to be 1.7 km².
22
23
24
25
26

163 2. EXPERIMENTAL ANALYSIS

164 2.1 Available data

165 Precipitation and temperature data are available from the Hemmingford weather station located
166 11 km from the peatland (Environment Canada, 2010). From 2007 to 2010, the annual average
167 precipitation was 1064 mm and the average annual temperature was 6.8°C. Snow usually falls
168 between November and March. Potential evapotranspiration (PET) is calculated with the Oudin et
169 al. (2005) equation. This equation provides PET estimates based on mean daily air temperature
170 and on extraterrestrial radiation which is estimated following Morton (1983). The seasonal net
171 precipitation (precipitation - PET) is estimated for three-month periods between 2007 and 2010
172 (Table 1). It varies from a negative net precipitation in summer to a winter maximum of 285 mm.
173 A negative net precipitation indicates seasons where potential evapotranspiration could not be
174 met by precipitation. Because of the sub-zero temperatures, the winter net precipitation
175 accumulates on the ground as snow and becomes available only during spring snowmelt. The
176 average annual PET calculated with the Oudin equation from 2007 to 2010 was 664 mm y⁻¹. The

1
2
3 177 average net precipitation is therefore 400 mm y^{-1} for this period and varies from 323 to 567 mm y
4
5 178 ¹.

7 179 Figure 1a shows the location of gauging stations and their contributing watersheds in the Covey
8
9 180 Hill Natural Laboratory where water levels have been recorded hourly since 2007 (*Trutrack* level
10
11 181 loggers) on the Allen River (29 km² watershed) and the Outardes River (26 km² watershed) as
12
13 182 well as on the Schulman stream (2.7 km² watershed). For all gauging stations, rating curves were
14
15 183 constructed by measuring flow rates manually (*Swoffer2100* velocimeter). Flows were estimated
16
17 184 during the frost free period of May to October from 2007 to 2010 (2007 to 2009 for the Schulman
18
19 185 stream). The Chapman (1999) digital filter was used on the flow rate time series to separate
20
21 186 baseflows from total flows (see Table 1). Without field calibration it is difficult to determine the
22
23 187 baseflow recession constant k , which describes the rate of baseflow decay. Here, a k value of
24
25 188 0.99 was used to represent the relatively low groundwater contribution to river flows (cf. Gagné,
26
27 189 2010). Total flows and baseflows are similar for the Allen and Outardes rivers and are an order of
28
29 190 magnitude smaller for the Schulman stream, as expected when comparing watershed sizes (see
30
31 191 Figure 1). On average, the estimated baseflows represent 39, 27 and 29% of the total flows for the
32
33 192 Allen River, the Outardes River and the Schulman stream respectively. These proportions are
34
35 193 relatively small, but typical of values found in headwater streams (e.g. Croteau et al., 2010). The
36
37 194 proportionately larger baseflows on the Allen River can be explained by the presence of deep
38
39 195 lakes along its course that intercept significant volumes of groundwater and smooth the impact of
40
41 196 rain events.
42
43
44
45

46 197
47
48 198 Groundwater levels were measured in two bedrock piezometers located near the peatland (4.5 and
49
50 199 15 m depth), in nine private monitoring wells, and in three observation wells owned by the
51
52 200 Geological Survey of Canada (*Solinst* level loggers; hourly measurements year round). A total of
53
54 201 371 heads are also available from a provincial water well database, the Système d'informations
55
56 202 hydrogéologiques (SIH) (Ministère du Développement durable, de l'Environnement, de la Faune
57
58
59
60

1
2
3 203 et des Parcs-MDDEFP, 2010). Six piezometers (approximately 0.5 m depth) are located directly
4
5 204 in the peatland to monitor groundwater levels in the organic deposits (*INW-PT2X* level loggers;
6
7 205 hourly measurements during the frost free period of May to October). Several of these
8
9
10 206 piezometers and the shallow bedrock observation well are depicted in Figure 1b. The bedrock
11
12 207 water table is located near the surface (between 2 and 15 m depth). Groundwater flows generally
13
14 208 in a radial direction from the hilltop, in the laterally-extensive fractures and dissolution joints
15
16 209 rather than in the sandstone porosity (Nastev et al., 2008). Heads in the peatland are lower than in
17
18 210 the surrounding bedrock aquifer, indicating lateral groundwater input from the aquifer to the
19
20 211 peatland (Fournier, 2008).
21
22
23
24

25 213 Hydraulic conductivity (K) values for the fractured bedrock are available from pumping tests and
26
27 214 packer tests reported in previous studies (Barrington et al., 1992; Lavigne et al., 2010a) and from
28
29 215 slug tests performed in the two bedrock observation wells located near the peatland (Fournier,
30
31 216 2008). Available data for bedrock K range from 4×10^{-10} to 1×10^{-4} m s⁻¹. These highly variable
32
33 217 values correspond to a wide range of fracture apertures and connectivity, but clearly decrease
34
35 218 with depth. Peat hydraulic conductivity was estimated by Fournier (2008). For the top 0.3 m, it
36
37 219 was estimated using an experimental tank reproducing Darcy's experiment (Rosa and Larocque,
38
39 220 2008) and varies between 0.00189 and 0.00725 m s⁻¹. Below this depth and down to 1 m, it was
40
41 221 estimated with the Modified Cubic Method (Beckwith et al., 2003a) and varies between 2.1×10^{-8}
42
43 222 and 1×10^{-4} m s⁻¹. Hydraulic conductivities show a significant decreasing pattern with depth.
44
45 223 Below 1 m, K is expected to be very low and probably significantly restricts flow in the lower
46
47 224 peat layers.
48
49
50
51
52

53 226 ***2.2 Development of the groundwater flow model***

55 227 The MODFLOW software (Harbaugh, 2005) was used to simulate groundwater flow in the
56
57 228 fractured bedrock and interactions between the aquifer, the peatland and streams, assuming that
58
59
60

1
2
3 229 the unconfined bedrock aquifer behaves as an equivalent porous medium. A digital elevation
4
5 230 model was built using elevation data from the Ministère des Ressources Naturelles (MRNF,
6
7 231 2007). The groundwater flow model is discretized in 16 layers for a total thickness of 96 m (layer
8
9 232 thickness increases from 0.25 m at the surface to 30 m at the base of the aquifer). The upper eight
10
11 233 layers are thin to allow an accurate representation of the peatland stratigraphy: the top two layers
12
13 234 (each 0.25 m thick) correspond roughly to the top portion of the acrotelm while the next layers
14
15 235 correspond to gradually more humified and less permeable peat layers (reaching the catotelm). A
16
17 236 variable head representation of the peatland was used rather than a constant head boundary
18
19 237 condition to ensure that simulated flows reflect the hydraulic properties of both the bedrock and
20
21 238 the organic deposits in changing hydrological conditions. This representation of the organic
22
23 239 deposits is nevertheless simplified and does not include lateral heterogeneity within the peat
24
25 240 deposits which can drive groundwater flow (Beckwith et al., 2003b).

26
27 241
28
29 242 The model extends north and east from Covey Hill into the St. Lawrence Lowlands and covers a
30
31 243 total area of 173 km². It is limited to the northwest by the Outardes River and to the north by the
32
33 244 Noire River (Figure 2). A specified head boundary is used to allow groundwater flow to the
34
35 245 regional aquifer. A no-flow boundary is used approximately 9 km parallel to and east of the Allen
36
37 246 River. This is a flow line based on the piezometric map. The southern and southwestern limit is
38
39 247 set on the drainage basins of the Allen and Outardes rivers (i.e., a water-divide, thus a no-flow
40
41 248 boundary is used). The bedrock at the base of the model is a no-flow boundary. The model
42
43 249 consists of 9698 cells of 135 m x 135 m. Cells are refined over and around the peatland
44
45 250 (67.5 m x 67.5 m) to ensure a good representation of head variations. Figure 3 presents a three-
46
47 251 dimensional depiction of the model, with a vertical exaggeration of 10 times.

48
49 252
50
51 253 The Outardes and Allen rivers are represented using MODFLOW's River package in the top two
52
53 254 layers. The Blueberry Lake and the Gouffre Lake, as well as a marsh area in the USA portion of
54
55
56
57
58
59
60

1
2
3 255 the Allen River are set as constant heads. Small permanent streams and tributaries are represented
4
5 256 using MODFLOW's Drain package in the top two layers. Recharge zones are determined
6
7 257 according to the slope and type of Quaternary deposits (Figure 2a, Table 2). The study area is
8
9 258 divided into four hydraulic conductivity zones (Figure 2b). Zone 1 corresponds to the peatland.
10
11 259 The Covey Hill formation is divided into three zones (2, 3 and 4) based on areas of similar
12
13 260 elevation and field hydraulic conductivity measurements (Lavigne et al., 2010a).
14
15
16 261
17
18 262 The model was calibrated in steady-state by manually adjusting the K values of the four hydraulic
19
20 263 conductivity zones using a trial and error procedure based on measured K data. Zonal recharge
21
22 264 and river and stream exchange coefficients were also calibrated. The storage coefficient for the
23
24 265 organic deposits (zone 1) was set to 0.7, based on an estimation from water level increases
25
26 266 following precipitation events (Fournier, 2008) and was calibrated for the bedrock hydraulic
27
28 267 conductivity zones. The calibration targets are the available head measurements (SIH database,
29
30 268 bedrock observation wells, private monitoring wells and peatland piezometers) as well as the
31
32 269 baseflows estimated for the three gauging stations (Allen and Outardes rivers, Schulman stream).
33
34
35 270
36
37 271 In transient-state, the year is divided into four stress periods of 91 days (10 time steps in each
38
39 272 period) corresponding to spring, summer, fall and winter. Following a 20 year spin-up period, the
40
41 273 transient model was executed to simulate the 2007-2010 flows, the period during which detailed
42
43 274 transient hydrological data are available. In MODFLOW, multipliers are used to modify the value
44
45 275 of calibrated steady-state recharge for each transient period. These multipliers were calculated for
46
47 276 each 91 day season using the ratio of the net precipitation for the season of interest to the average
48
49 277 net precipitation for the calibrated steady-state period. This method assumes that seasonal
50
51 278 recharge is distributed analogously to the net precipitation ratios. That is, a lower net precipitation
52
53 279 will lead to a reduction in both runoff and infiltration. The same multipliers were used for all
54
55 280 recharge zones. In the model, the winter recharge is set to zero and transferred to the spring
56
57
58
59
60

1
2
3 281 (when net precipitation is therefore usually the highest). For periods where the net precipitation is
4
5 282 a negative value (i.e. for some summer periods), the recharge in the model is also set to zero.
6
7
8 283

9 284 *2.3 Climate change scenarios*

10 285 The impact of climate change on groundwater recharge was investigated by considering net
11
12 286 precipitation values calculated with future time series of daily precipitation and temperature data.
13
14 287 It is assumed that recharge will follow the same pattern as net precipitation, such that a lower net
15
16 288 precipitation will lead to an analogous reduction in both runoff and infiltration. This might not
17
18 289 hold true if rainfall intensity increases or if there is less snow due to a shorter winter. Predicted
19
20 290 PET values were derived from Regional Climate Models (RCMs) future temperature time series
21
22 291 used in the Oudin et al. (2005) equation. Although using a daily weather generator and a recharge
23
24 292 model might provide more detailed input data for the groundwater flow model (cf. Herrera-
25
26 293 Pantoja et al., 2011), it would be much more labor intensive and is beyond the scope of this work.
27
28
29
30
31
32

33 295 The climate change scenarios are derived from four RCMs driven by six General Circulation
34
35 296 Models (GCMs). This form of dynamic downscaling provides a better representation of both
36
37 297 average conditions and extremes than other methods over the study area. Future RCM scenarios
38
39 298 were further downscaled using the daily translation bias correction method (Mpelasoka and
40
41 299 Chiew, 2009) to remove the biases between simulated and observed temperature and precipitation
42
43 300 variables.
44
45
46
47

48 302 Ten projections (Figure 4, Table 3) were selected from the 25 dynamically downscaled
49
50 303 simulations available for the Covey Hill area. Most of the simulations are outputs of the Canadian
51
52 304 Regional Climate Model (CRCM) (Music and Caya, 2007) and were generated and supplied by
53
54 305 the Ouranos Consortium on Regional Climatology and Adaptation to Climate Change. The
55
56 306 remaining simulations are from the North American Regional Climate Change Assessment
57
58
59
60

1
2
3 307 Program. All projections are for the 2041-2070 climate. The 10 simulations account for 85% of
4
5 308 the future climate variability projected for the study site as established by a cluster analysis
6
7 309 carried out on the range of available RCM scenarios. The simulations are driven by six different
8
9 310 GCMs under the Intergovernmental Panel on Climate Change emissions scenarios A1B and A2
10
11 311 (IPCC, 2000). The A1B emissions scenario corresponds to a medium population growth, rapid
12
13 312 gross domestic product growth and a balance of all energy sources. The A2 scenario is based on
14
15 313 high population growth, medium gross domestic product growth, high energy use, medium-to-
16
17 314 high land-use changes, and slow introduction of more energy efficient technologies. The A2
18
19 315 scenario is one of the most commonly used scenarios (Jackson et al., 2011).
20
21
22 316
23
24 317 Future RCM scenarios predict annual average air temperatures increasing by 2.4°C
25
26 318 (CRCM4.2.3_ECHAM#1) to 3.6 °C (CRCM4.2.3_CGCM3#2) for the 2041-2070 period. These
27
28 319 temperature increases far exceed the maximum difference of 1.6°C from the mean annual
29
30 320 temperature observed from 1971 to 2000 on Covey Hill. When used in the Oudin et al. (2005)
31
32 321 formula, the increased temperatures of the climate scenarios induce 15 to 21% increase in
33
34 322 predicted PET compared to the PET value of the reference period. Annual precipitation
35
36 323 projections range from a 3% increase (CRCM_CCSM) to a 13% increase (ECP2_GFDL). This
37
38 324 range of precipitation variation is small when compared to the -19% to +38% difference from the
39
40 325 mean precipitation observed from year to year during the reference period.
41
42
43 326
44
45 327 Stemming from these changes in temperature and precipitation, net precipitation varies from a
46
47 328 30% decrease (CRCM_CCSM) to a 10% increase (CRCM4.2.3_ECHAM#1). The net
48
49 329 precipitation scenarios do not all agree about the sign of change: seven predict a decrease in mean
50
51 330 net precipitation and three an increase. The bounds of the bootstrapped 95% confidence interval
52
53 331 on the ensemble mean are -21.5% and 2.9%. The sign of change for net precipitation thus remains
54
55 332 uncertain. To facilitate simulations, groundwater recharge variations of +10%, -15% and -30% of
56
57
58
59
60

1
2
3 333 the calibrated values are used to study the sensitivity of peatland-aquifer interactions under
4
5 334 climate change. These percentages are a simplification of the complex multi-scenario possibilities
6
7 335 but are considered sufficiently representative to generate informative results. In the literature,
8
9 336 recharge variations due to climate change for humid areas are expected to differ significantly
10
11 337 depending on topography, geology and climate. The recharge variations used here are similar to
12
13 338 those reported in literature: -59 to +15% in the Chateauguay watershed (Croteau et al., 2010),
14
15 339 +53% in the Grand River watershed of Ontario, Canada (Jyrkama and Sykes, 2007), +11 to +25%
16
17 340 in the Grand Forks aquifer of British Columbia, Canada (Scibek et al., 2007), -40 to +31% for
18
19 341 various locations in Great Britain (Herrera-Pantoja and Hiscock, 2008; Jackson et al., 2011). In
20
21 342 the semi-arid region of the southern High Plains of Texas, USA, Ng et al. (2010) report climate
22
23 343 change induced groundwater recharge variations from -75% to +35%.
24
25
26
27 344

28 29 345 **3. RESULTS AND DISCUSSION**

30 31 346 *3.1 Model calibration, measured and simulated baseline conditions*

32
33 347 The calibrated K_s in the groundwater model are within the interval of measured values
34
35 348 (Barrington et al., 1992; Fournier, 2008; Lavigne et al., 2010a), decreasing with depth as
36
37 349 observed with field measured data (Figure 5). The calibrated K in the peatland is high in the top
38
39 350 two layers of organic deposits and decreases rapidly below this depth. Below these layers K is set
40
41 351 to even lower values to represent gradually more humified and less permeable peat. The K_h/K_v
42
43 352 ratio in bedrock layers 1-9 of zones 2 and 3 is set to 1000 and 100 respectively, to represent the
44
45 353 predominantly horizontal groundwater flow within the horizontal bedding planes. The K_h/K_v ratio
46
47 354 layers 10-12 for zones 1, 2 and 3 are set to 100, and the deeper anisotropy for these zones is set to
48
49 355 10. In zone 4, the K_h/K_v ratio is 10 for all layers. The calibrated conductance for the River nodes
50
51 356 is $200 \text{ m}^2 \text{ d}^{-1}$. This value provides the best estimates of river base flows. Calibrated conductance
52
53 357 for the drains is $500 \text{ m}^2 \text{ d}^{-1}$.
54
55
56
57 358

1
2
3 359 For the steady-state simulation, the maximum possible recharge was limited to the average annual
4
5 360 net precipitation for the 2007-2012 period (400 mm y⁻¹). The steady-state calibrated average
6
7 361 recharge for the entire domain is 113 mm y⁻¹, i.e. 28% of this average net precipitation. The
8
9
10 362 difference between net precipitation and recharge can be justified by the diversion of net
11
12 363 precipitation to streams and evacuated via surface routes (not simulated in this work). Spatially
13
14 364 calibrated recharge varies between 0 and 372 mm y⁻¹ (Table 2). The maximum value is attributed
15
16 365 to the peatland where little runoff occurs. The minimum recharge is calibrated on the northern
17
18 366 portion of the study area where compact till, silt and clay sediments are found. Although in reality
19
20 367 recharge is rarely nil, this value illustrates the very limited water volumes that can percolate
21
22 368 through these low permeability sediments. The calibrated recharge obtained in this study is lower
23
24 369 than the values of 162-180 and 227-240 mm y⁻¹ previously estimated by Croteau et al. (2010) and
25
26 370 Gagné (2010) respectively for the Allen and Outardes watersheds. This difference can be
27
28 371 attributed to the fact these authors calibrated recharge using soil reservoir models to reproduce
29
30 372 baseflow estimated from hydrograph separation. Because it is very difficult to distinguish
31
32 373 between recharge and subsurface runoff with hydrograph separation, this method can
33
34 374 overestimate actual recharge to the aquifer.
35
36
37
38
39

40 376 For the transient state simulations, Table 1 presents the seasonal values of recharge. Seasonal
41
42 377 recharge is lowest (almost zero) in summer and largest in the spring due to snowmelt. From 2007
43
44 378 to 2010, the annual recharge varies from 98 to 172 mm y⁻¹. The storage coefficient was calibrated
45
46 379 to 0.004 for the bedrock in zone 2, and 0.001 in zones 3 and 4, typical values for fractured
47
48 380 bedrock (Anderson and Woessner, 1992).
49

50 381
51
52
53 382 Figures 6a and b show that the steady-state groundwater flow model simulates the available head
54
55 383 data without any systematic overestimation or underestimation of heads in any area of the study
56
57 384 domain (mean error 0.4 m, mean absolute error 7.2 m and root mean squared error 9.3 m). The
58
59
60

1
2
3 385 simulated errors can be partially explained by the fractured and probably highly heterogeneous
4
5 386 bedrock aquifer, a condition not represented with the equivalent porous media model. The error
6
7 387 on the simulated heads could also arise from the inaccuracy of the SIH data, because it is
8
9 388 measured over several years, there are variable drilling depths, and the reference topography
10
11 389 (which itself is highly varied) is estimated, and from the inaccuracy in the elevation model.
12
13 390 Nevertheless, the calibrated model simulates the large head differences observed over this
14
15 391 headwater area relatively well.
16
17 392
18
19 393 Figure 7 illustrates measured and simulated heads from 2007 to 2010 for the peatland and three
20
21 394 wells located at the top of the hill, at mid-slope, and at the foot of the hill. The heads are plotted
22
23 395 relatively (i.e. elevation centered on 0) to remove any errors related to topographical inaccuracies.
24
25 396 The simulated groundwater levels compare reasonably with the observation data. For example,
26
27 397 the Nash-Sutcliffe efficiency coefficient (Nash and Sutcliffe, 1970), comparing the seasonal
28
29 398 bedrock observation well heads to the simulated heads, where $E = 1$ corresponds to a perfect
30
31 399 match, ranges from 0.983 to 0.998 for the illustrated wells and is similar for the additional
32
33 400 bedrock monitoring wells. For the peatland piezometers, the efficiency coefficients are similar
34
35 401 (e.g. 0.994 as illustrated in Figure 7). Errors in the transient state simulation are expected to be
36
37 402 caused in part by the porous media representation of the fractured bedrock aquifer and the
38
39 403 imprecision in storage coefficient calibration.
40
41
42
43
44
45
46
47
48
49
50
51
52
53
54
55
56
57
58
59
60

405 Table 1 shows that the magnitudes of seasonal baseflows are relatively well simulated for the
406 Allen and Outardes rivers, and for the Schulman stream. Model baseflows range from 0.08 to
407 0.20 m³/s for the Allen, 0.05 to 0.24 m³/s for the Outardes and 0.006 to 0.014 m³/s for the
408 Schulman . However, the simulated values generally vary less from year to year than the
409 Chapman estimated baseflows. This could be due to the modeling methodology in which bulk
410 seasonal recharge values are used on three month stress periods, rather than storm-specific

1
2
3 411 precipitation and recharge extremes encountered in nature. Also, it must be remembered that the
4
5 412 Chapman estimated baseflows are only crude estimations of the aquifer contribution to the rivers.
6
7 413 Considering the simple representation of the groundwater contribution to rivers, these results are
8
9 414 considered satisfactory.
10
11 415
12
13 416 Fournier (2008) has estimated the groundwater flow contribution to the peatland using the Darcy
14
15 417 equation with bedrock-peatland head gradients and measured hydraulic conductivities. The same
16
17 418 technique was used here on a seasonal basis. The average seasonal hydraulic gradient between the
18
19 419 4.5 m bedrock piezometer located near the peatland and the closest peatland piezometer is used in
20
21 420 this calculation. During the 2007-2010 period, this hydraulic gradient was on average slightly
22
23 421 higher during the spring (0.0032 m/m), a mid-value during the fall (0.0031 m/m) and lowest
24
25 422 during the summer (0.0029 m/m). It is assumed to be constant all along the 5580 m of the aquifer-
26
27 423 peatland North and South inflow lengths. The hydraulic conductivity corresponds to the average
28
29 424 between 4.5 m bedrock piezometer K (3.54×10^{-5} m/s) and the hydraulic conductivity of the
30
31 425 topmost 0.5 m of peat deposits (1.84×10^{-3} m/s). The model simulates groundwater inflows to the
32
33 426 peatland (Table 1) similar to the Darcy flux values for the spring (0.0072 for the model vs. 0.0082
34
35 427 m^3/s for Darcy), but lower for the summer (0.0037 vs. 0.0076 m^3/s) and fall (0.0053 vs. 0.0080
36
37 428 m^3/s) seasons. Although relatively small, this groundwater inflow to the peatland is nevertheless
38
39 429 important for the hydrological dynamics of the peatland, its ecosystem and habitat diversity. This
40
41 430 inflow provides sustained minerals, nutrients and water to maintain rich and diverse plant
42
43 431 communities identified in the minerotrophic transition zone (lagg ecotone; Pellerin et al. 2009).
44
45 432 The direction of groundwater flow (i.e. always from aquifer to peatland under current climate
46
47 433 conditions) is also correctly simulated. Because of the significantly higher hydraulic
48
49 434 conductivities in the upper peat layers, the model simulates groundwater movement through the
50
51 435 peatland mainly in the topmost 0.5 m. Similar dominating superficial flow within the top layers of
52
53 436 a peatland has also been reported in other field studies (e.g. Devito et al., 1996).
54
55
56
57
58
59
60

1
2
3 437 The model predicts groundwater outflow from the peatland in the direction of the Allen and
4
5 438 Outardes rivers, equivalent to 4 to 7% of the total baseflow to each river. Simulated flows from
6
7 439 the peatland to the two rivers are largest during the spring and fall seasons with a total out flow of
8
9 440 0.0157 and 0.0131 m³/s respectively for the two seasons. Outflows remains non-negligible (under
10
11 441 current conditions) throughout the year (minimum 0.0102 m³/s during the winter) , with highest
12
13 442 contributing percentages in summer and winter when river baseflows are the lowest. Other studies
14
15 443 (e.g. Devito et al., 1997) have shown that baseflow from a headwater peatland can be interrupted
16
17 444 during the dry season in a low permeability headwater bedrock settings. Although the
18
19 445 groundwater flow model for Covey Hill does not provide detailed information on river baseflows,
20
21 446 the simulations show that the storage-release capacity of the peatland is important to support river
22
23 447 low flows. Similarly to other headwater peatlands, the Covey Hill peatland appears to play a
24
25 448 significant buffer role in a hydrological system where the soil and surface deposits offer little
26
27 449 storage potential to maintain river flows during the dry season.
28
29
30

31 450
32
33 451 Twelve percent of the recharge applied to the model domain is discharged from the aquifer to the
34
35 452 small streams which are represented by drains. This corresponds to a significant volume of water,
36
37 453 of a similar magnitude to the simulated baseflows of the Allen or the Outardes River. Thirty
38
39 454 percent of the recharge emerges in the Allen and Outardes rivers as well as in the Schulman
40
41 455 stream upstream from the gauging stations (see Figure 1). Twelve percent emerges in the two
42
43 456 rivers below their gauging stations where the rivers flow mostly on impervious sediments and
44
45 457 have little interaction with the aquifer.
46
47
48

49 458
50
51 459 During an average year, the total flow to the regional aquifer through the northern boundary is
52
53 460 equivalent to 52 mm y⁻¹. This inter-aquifer flow represents 46% of the average calibrated
54
55 461 recharge for the study domain. Covey Hill is a recharge zone but small streams and rivers
56
57 462 intercept a significant part of this recharge. The volume of water that actually reaches the regional
58
59
60

1
2
3 463 aquifer is therefore much lower than what reaches the saturated zone. This is rarely taken into
4
5 464 consideration when evaluating regional recharge with 1D water budget methods. This proportion
6
7 465 of total recharge that reaches the regional aquifer as groundwater flow cannot be verified with
8
9
10 466 field measurements but appears reasonable given the other simulated flows. Comparatively, in a
11
12 467 nearby watershed in south-western Quebec, Nastev et al. (2006) found that discharge to
13
14 468 secondary streams comprised 37% of the water budget.
15

16 469

17 18 470 *3.2 Simulated climate change scenarios*

19
20 471 The recharge scenarios investigated in this study are considered a representative range of possible
21
22 472 recharge variations for a future climate. Although the 2007-2010 period during which detailed
23
24 473 transient hydrological data are available is outside the 1971-2000 reference period for the climate
25
26 474 change scenarios, the four recharge scenarios are simulated up to 2010 to facilitate comparison
27
28 475 with recent conditions.
29

30 476

31
32
33 477 Figure 8 illustrates variations in heads, river and stream flows, as well as subsurface outflow
34
35 478 through the northern boundary for each of the recharge scenarios relative to the spring 2010
36
37 479 baseline results. Trends are similar for data from other seasons and years. Recharge variations of
38
39 480 +10, -15 and -30% induce median head changes of +1.1, -1.9 and -4.2 m respectively. This high
40
41 481 sensitivity of groundwater levels to recharge variations is probably a common trait of headwater
42
43 482 aquifers and is an argument in favor of management measures that would limit human-induced
44
45 483 recharge reductions or wetland drainage in headwater systems. Nevertheless, the headwater
46
47 484 system apparently has some resilience, buffering recharge variations to a limited extent.
48

49
50 485 Interestingly, removing the peatland (i.e. zone 1) from the model in steady state, and therefore
51
52 486 simulating a major perturbation scenario, produces a reduction in heads similar to a 15% decrease
53
54 487 in recharge (results not shown). The water holding capacity of the organic deposits therefore
55
56 488 contributes to some extent to maintain high groundwater levels near the top of the Covey Hill
57
58
59
60

1
2
3 489 headwater system. In the absence of soils and surface deposits, the Blueberry, Gouffre and Forêt
4
5 490 Enchantée lakes certainly also contribute to the hydrological resilience of the system. Beyond a
6
7 491 certain level of recharge reduction, heads change more significantly (and this change is much
8
9 492 more variable in space), the largest changes being observed on the top of the hill. This agrees
10
11 493 with results from other studies (e.g. Lavigne et al., 2010b) which have shown that the highest
12
13 494 sensitivity of groundwater levels to pumping increases occurs in areas where potentiometric
14
15 495 heads are the highest.
16
17
18 496
19
20 497 Total contribution from the aquifer to the Allen and Outardes rivers, to the Schulman stream and
21
22 498 to all the small streams varies from +14% to -22 and -44% of the baseline for the +10%, -15%
23
24 499 and -30% recharge scenarios respectively (Figure 8). In the model, the Allen and Outardes rivers
25
26 500 never become dry because they are represented using MODFLOW's River package. This is
27
28 501 probably realistic since inputs from the peatland and from a series of lakes along their courses
29
30 502 provide significant reservoirs to maintain flow throughout the year. The Schulman stream and the
31
32 503 smaller streams located on the northern face of the hill simulated with the Drain package can
33
34 504 become seasonally isolated from the aquifer due to low piezometric levels, which represents
35
36 505 drying. When recharge decreases, small streams and springs dry out. This drying of small streams
37
38 506 and springs could have an adverse effect on endangered salamanders species found on Covey Hill
39
40 507 (Larocque et al., 2006).
41
42
43 508
44
45 509 As recharge decreases, the proportion of the recharge flowing to the regional aquifer increases
46
47 510 only slightly for the -15% and -30% scenarios respectively. As less water is diverted to surface
48
49 511 routes, more (proportionately) can flow to the regional aquifer. This comes from the drying out of
50
51 512 small streams that otherwise drain groundwater towards surface streams and rivers. Conversely, a
52
53 513 10% increase in recharge drives more water to rivers and drains and less, percentage wise, to the
54
55 514 regional aquifer.
56
57
58
59
60

1
2
3 515 During the 2007-2010 period, the peatland was constantly fed by the aquifer. Groundwater input
4
5 516 to the peatland increases with the +10% recharge scenario, leading to an increase in heads and to
6
7 517 more water drained by the peatland outlets. When recharge decreases by 15%, water flows from
8
9 518 the bedrock aquifer to the peatland on the southern portion and from the peatland to the aquifer
10
11 519 on its northern side (Figure 9). Outflows from the peatland are even higher for the -30% recharge
12
13 520 scenario. Also, oxidation of peat and vegetation changes could also occur in response to reduced
14
15 521 groundwater inflow to the peatland. Extrapolating from a trend line for flow to the peatland from
16
17 522 the aquifer, a recharge decrease of 16.5% causes an annual net groundwater contribution to the
18
19 523 peatland of zero. Figure 10 shows that with the -30% recharge scenario, flow reversals occur
20
21 524 during the summer, fall and winter seasons, and sometimes during the spring. Under these
22
23 525 conditions, the flow regime changes and more water flows out of the peatland than into it through
24
25 526 most of the year. This could induce water table drawdowns within the peatland that are beyond
26
27 527 the threshold of peatland vegetation resilience to groundwater level variations. Significant
28
29 528 vegetation changes could result from this situation with tree growth increase and further reduction
30
31 529 of the organic matter accumulation within the peatland. Frequent or long term changes of this
32
33 530 nature could impair the buffer function of the headwater peatland. Conversely, with higher
34
35 531 recharge some areas of the peatland would become totally flooded. This could significantly
36
37 532 impact its vegetation favouring for instance the spread of minerotrophic marshes and aquatic
38
39 533 plants (Swan and Gill, 1970; Asada et al., 2005).
40
41
42
43
44
45
46
47
48
49
50
51
52
53
54
55
56
57
58
59
60

535 It is noteworthy to underline the fact that detailed representation of recharge fluxes and changes
536 in the seasonal occurrence of recharge are not included in this study. This is especially true for
537 winter conditions. Under climate change, the RCM scenarios predict higher winter temperatures,
538 with a mean temperature change of +3.1°C, ranging from +2.1°C to +4.2°C. This will lead to a
539 shorter period of below zero temperatures (10 to 14 days), more frequent recharge events during
540 the winter season, reduced snow accumulation and reduced spring recharge. The climate models

1
2
3 541 indicate an increase in rainfall intensity with the 90th percentile of the maximum daily
4
5 542 precipitation rising from 63.7 to 72.7 mm. A detailed soil water budget model would have been
6
7 543 necessary along with monthly (or shorter) stress periods to illustrate in more details the impact of
8
9 544 increased winter recharge or rainfall intensity on local and regional groundwater flow.
10
11 545

12
13
14 546 For the two recharge reduction scenarios, the peatland groundwater contributing area is mostly
15
16 547 located at the southwest of the peatland and is reduced from 1.7 km² to 1.2 and 1.1 km²
17
18 548 respectively. As mentioned above, the peatland watershed is relatively small and influenced only
19
20 549 by local groundwater flow. In this respect, the Covey Hill peatland is probably typical of
21
22 550 peatlands located in headwater systems where undulating topography limits the area contributing
23
24 551 to groundwater flow. This situation makes it particularly sensitive to hydrological changes in
25
26 552 rainfall and recharge.
27
28 553

29 554 **4. CONCLUSION**

30
31
32
33 555 This work provides insights into the hydrological functions of a headwater system and peatland in
34
35 556 regulating groundwater levels and river baseflows. Under current conditions, this work confirms
36
37 557 that the Covey Hill peatland is fed by the fractured bedrock aquifer year round and provides
38
39 558 continuous baseflow to its outlets. A peatland located in a headwater system where surface
40
41 559 deposits are scarce is expected to play an important role as a water reservoir, helping to regulate
42
43 560 the impacts of climate variability. A suite of Regional Climate Model scenarios have provided a
44
45 561 net precipitation variation range from -30% to +10% for the 2041-2070 horizon. This range was
46
47 562 used to modify calibrated recharge values. Over the studied headwater system, recharge
48
49 563 reductions induce sharp declines in groundwater levels and drying streams. Recharge variations
50
51 564 of +10, -15 and -30% induce median head changes of +1.1, -1.9 and -4.2 m respectively. Close to
52
53 565 the peatland and within the organic deposits, hydraulic gradients change and the peatland
54
55 566 becomes perched above the aquifer during the summer, fall and winter. Although the climate
56
57
58
59
60

1
2
3 567 change induced recharge scenarios tested in this work are hypothetical, results from this study
4
5 568 indicate that a headwater system can be highly vulnerable to recharge variations, both in terms of
6
7 569 heads and fluxes. Although the knowledge exists to link these trends to ecosystem changes, more
8
9 570 work is needed to establish specific thresholds and quantifiable ecological responses.
10

11 571

12
13
14 572 The MODFLOW model has proven to be adequate to simulate current groundwater flow
15
16 573 conditions in both steady and transient states in the Covey Hill headwater bedrock aquifer as well
17
18 574 as to simulate interactions between aquifer and peatland. This was achieved in spite of the
19
20 575 inevitable simplifications necessary to represent a regional aquifer, namely using an equivalent
21
22 576 porous media representation for the fractured bedrock and deriving recharge from net
23
24 577 precipitation values. Representing the peatland explicitly and not overly constraining it using, for
25
26 578 example, a constant head boundary condition, was necessary to study the peatland-aquifer
27
28 579 interactions. In further research based on additional field characterization, using a fully coupled
29
30 580 model could allow the simulation of runoff and infiltration as specific processes, as well as the
31
32 581 simulation of surface flow to rivers.
33
34

35 582

36
37
38 583 In this study, recharge variations were related to climate change. Other human-induced recharge
39
40 584 variations can result from increased urbanization or groundwater level decreases due to
41
42 585 groundwater abstraction to meet agricultural or urban needs. The hydrogeological impact of these
43
44 586 variations could be magnified if combined with climate change induced recharge reductions.
45

46 587 Under these conditions, current management practices might not be sufficient to ensure the long
47
48 588 term hydrological and ecosystem functions of a headwater system. More research is necessary to
49
50 589 include these considerations into management practices to develop adaptation strategies in the
51
52 590 anticipation of climate change and population growth.
53
54

55 591

56
57 592
58
59
60

1
2
3 593 **ACKNOWLEDGEMENTS**
4

5 594 This project was funded by the climate change consortium Ouranos as part of the "Fonds vert" for
6
7 595 the implementation of the Quebec Government Action Plan 2006-2012 on climate change
8
9 596 (grant #554007 – 107). The authors would like to thank Nature Conservancy of Canada for its
10
11 597 logistic contribution and for providing access to its property on Covey Hill. We also thank the
12
13 598 landowners for making their properties accessible for the study.
14
15

16 599
17

18 600
19
20
21
22
23
24
25
26
27
28
29
30
31
32
33
34
35
36
37
38
39
40
41
42
43
44
45
46
47
48
49
50
51
52
53
54
55
56
57
58
59
60

For Peer Review

601 **REFERENCES**

- 602 Ackerman MC, Blake JR, Booker DJ, Harding RJ, Reynard N, Mountford JO, Stratford CJ. 2009.
603 A simple framework for evaluating regional wetland ecohydrological response to climate
604 change with case studies from Great Britain. *Ecohydrology* doi:10.1002/eco.37.
- 605 Anderson MP, Woessner WW. 1992. Applied groundwater modeling: simulation of flow and
606 advective transport. *Academic Press, Inc.*, San Diego, California, 381 p.
- 607 Asada T, Warner BG, Schiff SL. 2005. Effects of shallow flooding on vegetation and carbon
608 pools in boreal peatlands. *Applied Vegetation Science* **8**:199–208.
- 609 Baird AJ, Morris PJ, Belyea LR. 2011. The DigiBog peatland development model 1: rationale,
610 conceptual model, and hydrological analysis. *Ecohydrology* doi:10.1002/eco.230.
- 611 Barrington S, Phillion H, Bonin J. 1992. An evaluation of the water reserve potentials : the
612 ecological region of the Covey Hill « Gulf ». Agricultural Engineering report, Faculty of
613 Agriculture and Environmental Sciences, *McGill University*, McDonald campus, 53 p.
- 614 Beckwith CW, Baird AJ, Heatwaite AL. 2003a. Anisotropy and depth-related heterogeneity of
615 hydraulic conductivity in a bog peat. I: laboratory measurements. *Hydrological Processes*
616 **17**:89-101.
- 617 Beckwith CW, Baird AJ, Heatwaite AL. 2003b. Anisotropy and depth-related heterogeneity of
618 hydraulic conductivity in a bog peat. II: modeling the effects on groundwater flow.
619 *Hydrological Processes* **17**:103-113.
- 620 Belyea LR, Malmer N. 2004. Carbon sequestration in peatlands: patterns and mechanisms of
621 response to climate change. *Global Change Biology* **10**:1043-1052.
- 622 Brassard P, Waddington MJ, Hill AR, Roulet NT. 2000. Modelling groundwater-surface water
623 mixing in a headwater wetland: implication for hydrograph separation. *Hydrological*
624 *Processes* **14**:2697-2710.
- 625 Calmé S, Desrochers A, Savard, JPL. 2002. Regional significance of peatlands for avifaunal
626 diversity in southern Quebec. *Biological Conservation* **107**:273-281.

- 1
2
3 627 Chapman, T. 1999. A comparison of algorithms for stream flow recession and baseflow
4
5 628 separation. *Hydrological Processes* **13**:01-714.
6
7 629 Cook PG. 2003. A guide to regional groundwater flow in fractured rock aquifers. CSIRO Land
8
9 630 and water, Glen Osmond, SA, Australia, 115 p.
10
11 631 Croteau A, Nastev M, Lefebvre R. 2010. Groundwater recharge assessment in the Châteauguay
12
13 632 River watershed. *Canadian Water Resources Journal* **35**(4):451-468.
14
15 633 Devito KJ, Waddington MJ, Branfireun BA. 1997. Flow reversals in peatlands influenced by
16
17 634 local groundwater systems. *Hydrological Processes* **11**:103-110.
18
19 635 Devito KJ, Hill AR, Roulet N. 1996. Groundwater-surface water interactions in headwater
20
21 636 forested wetlands of the Canadian Shield. *Journal of Hydrology* **181**:127-147.
22
23 637 Devito KJ. 1995. Sulphate mass balances in headwater wetlands of the Canadian Shield:
24
25 638 influence of catchment hydrogeology. *Canadian Journal of Fisheries and Aquatic Science*
26
27 639 **52**:1750-1760.
28
29 640 Ducks Unlimited Canada. 2006. Plan de conservation des milieux humides et de leurs terres
30
31 641 hautes adjacentes de la région administrative du Centre-du-Québec,
32
33 642 [<http://www.canardsquebec.ca>], 55 p.
34
35 643 Environment Canada. 2010. Moyenne climatique de la station Hemmingford Four winds Québec,
36
37 644 1961-2009. <http://www.climate.weatheroffice.ec.gc.ca/climateData/dailydata>.
38
39 645 Fournier V. 2008. Hydrologie de la tourbière du mont Covey Hill et implications pour la
40
41 646 conservation. M.Sc. thesis, *Université du Québec à Montréal*, 84 p.
42
43 647 Franzi D, Rayburn JA, Yansa CH, Knuepfer PLK. 2002. Late glacial water bodies in the
44
45 648 Champlain and Hudson lowlands, New York. In: *New York State Geological*
46
47 649 *Association/New England Intercollegiate Geological Conference Joint Annual Meeting*
48
49 650 *Guidebook*, pp. A5 1-23.
50
51 651 Gagné S. 2010. Contribution de l'eau souterraine aux cours d'eau et estimation de la recharge sur
52
53 652 le mont Covey Hill. M.Sc. Thesis *Université du Québec à Montréal*, 87 p.
54
55
56
57
58
59
60

- 1
2
3 653 Globensky Y. 1986. Géologie de la région de Saint-Chrysostome et de Lachine (sud). Ministère
4
5 654 de l'énergie et des ressources.
6
7 655 Greyson R, Holdon J, Rose R. 2010. Long-term change in storm hydrographs in response to
8
9 656 peatland vegetation change. *Journal of Hydrology* **389**:336-343.
10
11 657 Harbaugh AW. 2005. MODFLOW-2005, the U.S. Geological Survey modular ground-water
12
13 658 model -- the Ground-Water Flow Process: U.S. Geological Survey Techniques and Methods
14
15 659 6-A16, variously p. <http://pubs.usgs.gov/tm/2005/tm6A16/> .
16
17
18 660 Herrera-Pantoja M, Hiscock KM, Boar RR. 2011. The potential impact of climate change on
19
20 661 groundwater-fed wetlands in eastern England. *Ecohydrology* doi:10.1002/eco.231.
21
22 662 Herrera-Pantoja M, Hiscock KM. 2008. The effects of climate change on potential groundwater
23
24 663 recharge in Great Britain. *Hydrological Processes* **22**:73-86.
25
26
27 664 IPCC. 2000. Special report on emissions scenarios (SRES): A special report of working group III
28
29 665 of the intergovernmental panel on climate change. *Cambridge University Press*, Cambridge,
30
31 666 UK.
32
33 667 Jackson CR, Meister R, Prudhomme C. 2011. Modelling the effects of climate change and its
34
35 668 uncertainty on UK Chalk groundwater resources from an ensemble of global climate model
36
37 669 projections. *Journal of Hydrology* **399**:12-28.
38
39
40 670 Jyrkama MI, Sykes JF. 2007. The impact of climate change on spatially varying groundwater
41
42 671 recharge in the Grand River watershed (Ontario). *Journal of Hydrology* **338**:237-250
43
44 672 Kosugi K, Katsura S, Katsuyama M, Mizuyama T. 2006. Water flow processes in weathered
45
46 673 granitic bedrock and their effects on runoff generation in a small headwater catchment. *Water*
47
48 674 *Resources Research*, **42**, W02414, doi:10.1029/2005WR004275.
49
50
51 675 Lapen DR, Price JS, Gilbert R. 2005. Modelling two-dimensional steady-state groundwater flow
52
53 676 and flow sensitivity to boundary condition in blanket peat complexes. *Hydrological*
54
55 677 *Processes* **19**:371-386.
56
57
58
59
60

- 1
2
3 678 Larocque M, Leroux G, Madramootoo C, Lapointe FJ, Pellerin S., Bonin J. 2006. Mise en place
4
5 679 d'un laboratoires National sur le mont Covey Hill (Québec, Canada). *VertigO* 7 (1):1-11.
6
7 680 Lasalle P. 1981. Géologie des sédiments meubles de la région de St-Jean-Lachine. *Ministère de*
8
9 681 *l'Énergie et des Ressources du Québec*, Direction générale de l'exploration géologique et
10
11 682 minérale, DPV. 780.
12
13 683 Lavigne MA, Nastev M, Lefebvre R. 2010a. Numerical simulation of groundwater flow in the
14
15 684 Châteauguay River aquifers. *Canadian Water Resources Journal* 35(4):469-486.
16
17 685 Lavigne MA, Nastev M, Lefebvre R, Croteau A. 2010b. Regional sustainability of the
18
19 686 Châteauguay River aquifers. *Candian Water Resources Journal* 35(4):487-502.
20
21 687 MDDEFP (Ministère du Développement durable, de l'Environnement, de la Faune et des Parcs –
22
23 688 Québec). 2010. www.mddep.gouv.qc.ca/eau/souterraines/sih/index.htm.
24
25 689 Mearns LO, Arritt S, Biner M, Bukovsky S, Sain S, Caya D, Correia Jr J, Flory D, Gutowski W,
26
27 690 Takle ES, Jones R, Leung R, Moufouma-Okia W, McDaniel L, Nunes AMB, Qian Y, Roads
28
29 691 J, Sloan L, Snyder M. 2012. The North American Regional Climate Change Assessment
30
31 692 Program overview of phase I results. *Bulletin of the American Meteorological Society* 93:
32
33 693 1337-1362.
34
35 694 Moore PD. 2002. The future of cool temperate bogs. *Environmental Conservation* 29:3-20.
36
37 695 Morton FI. 1983. Operational estimates of areal evapotranspiration and their significance to the
38
39 696 science and practice of hydrology. *Journal of Hydrology* 66 (1-4):1-76.
40
41 697 Mpelasoka FS, Chiew FHS. 2009. Influence of rainfall scenario construction methods on runoff
42
43 698 projections. *Journal of Hydrometeorology* 10:1168-1183.
44
45 699 MRNF (Ministère des Ressources naturelles – Québec). 2007. Modèle d'élévation numérique
46
47 700 (10 m) de la région de St-Jean Chrysostome (1 : 20 000), 31H04-0101. Base de données
48
49 701 topographiques du Québec, Québec, Canada.
50
51
52
53
54
55
56
57
58
59
60

- 1
2
3 702 Music B, Caya D. 2007. Evaluation of the hydrological cycle over the Mississippi River Basin as
4
5 703 simulated by the Canadian Regional Climate Model (CRCM). *Journal of Hydrometeorology*
6
7 704 **8**:969-988.
8
9
10 705 Nash JE, Sutcliffe J V. 1970. River flow forecasting through conceptual models part I – A
11
12 706 discussion of principles. *Journal of Hydrology* **10**(3):282-290.
13
14 707 Nastev M, Morin R, Godin R, Rouleau A. 2008. Developing conceptual hydrological model for
15
16 708 Potsdam sandstones in southwestern Quebec, Canada. *Hydrogeology Journal* **16**:373-388.
17
18 709 Nastev M, Lefebvre R, Rivera A, Martel R. 2006. Quantitative assessment of regional rock
19
20 710 aquifers, south-western Quebec, Canada. *Water Resources Management* **20**:1-18.
21
22
23 711 Ng, G-H C, McLaughlin D, Entekhab, D, Scanlon BR. 2010. Probabilistic analysis of the effects
24
25 712 of climate change on groundwater recharge. *Water Resources Research* **46** W07502,
26
27 713 doi:10.1029/2009WR007904.
28
29
30 714 Oudin L, Hervieu F, Michel C, Perrin C, Andreassian V, Anctil F, Loumagne C. 2005. Which
31
32 715 potential evapotranspiration input for a lumped rainfall-runoff model? Part 2-Towards a
33
34 716 simple and efficient potential evapotranspiration model for rainfall-runoff modelling. *Journal*
35
36 717 *of Hydrology* **303**:290-306.
37
38 718 Parent M, Occhietti S. 1988. Late wisconsinian deglaciation and Champlain Sea invasion in the
39
40 719 St. Lawrence valley, Québec. *Géographie physique et Quaternaire* **42** :215-246
41
42 720 Pellerin S, Larocque M, Lavoie M, 2007. Rôle hydrologique et écologique régional de la
43
44 721 tourbière de Covey Hill. Report presented to the EJLB Foundation, 63 p.
45
46 722 Pellerin S, Lagneau LA, Lavoie M, Larocque M. 2009. Environmental factors explaining the
47
48 723 vegetation patterns in a temperate peatland. *C.R. Biologies* **332**:720-731.
49
50 724 Poulin M, Rochefort L, Pellerin S, Thibault J. 2004. Threats and protection for peatlands in
51
52 725 Eastern Canada. *Geocarrefour* **79**:331–344.
53
54
55
56
57
58
59
60

- 1
2
3 726 Reeve AS, Warzocha J, Glaser PH, Siegel DI. 2001. Regional ground-water flow modeling of the
4
5 727 Glacial Lake Agassiz Peatlands, Minnesota. *Journal of Hydrology* **243**:91-100.
6
7 728 Rosa E, Larocque M, Pellerin S, Gagné S, Fournier B. 2008. Determining the number of manual
8
9 729 measurements required to improve peat thickness estimations by ground penetrating radar.
10
11 730 *Earth Surface Processes and Landforms* doi:10.1002/esp.1741.
12
13 731 Rosa E, Larocque M. 2008. Investigating peat hydrological properties using field and laboratory
14
15 732 methods: application to the Lanoraie peatland complex (Southern Québec, Canada).
16
17 733 *Hydrological Processes* **22**:1866-1875.
18
19 734 Salinas MJ, Blanca G, Romero AT. 2000. Riparian vegetation and water chemistry in a basin
20
21 735 under semiarid mediterranean climate, Andarax River, Spain. *Environmental Management*
22
23 736 **26**(5):539-552.
24
25 737 Scibek J, Allen D, Cannon AJ, Whitfield PH. 2007. Groundwater-surface water interaction under
26
27 738 scenarios of climate change using a high-resolution transient groundwater model. *Journal of*
28
29 739 *Hydrology* **133**:165-181.
30
31 740 Strack M, Waddington MJ, Tuittila ES. 2004. Effect of water table drawdown on northern
32
33 741 peatland methane dynamics: Implications for climate change. *Global Biochem. Cy.* **18**:4003-
34
35 742 4010.
36
37 743 Swan JMA, Gill AM. 1970. The origins, spread, and consolidation of a floating bog in Harvard
38
39 744 Pond, Petersham, Massachusetts. *Ecology* **51**:829-840.
40
41 745 Tarnocai, C. 2006. The effect of climate change on carbon in Canadian peatlands. *Global*
42
43 746 *Planetary Change* **53**(4):222-232.
44
45 747 Tremblay T, Nastev M, Lamothe M. 2010. Grid-based hydrostratigraphic 3D modelling of the
46
47 748 Quaternary sequence in the Châteauguay River watershed, Quebec. *Canadian Water*
48
49 749 *Resources Journal* **35**(4):377-398.
50
51 750 Waddington JM, Quinton. WL, Price JS, Lafleur PM. 2009. Advances in Canadian peatland
52
53 751 hydrology, 2003-2007. *Canadian Water Resources Journal* **34**(2):139-148.
54
55
56
57
58
59
60

- 1
2
3 752 Whittington PN, Price JS. 2006. The effects of water table draw-down (as a surrogate for climate
4 change) on the hydrology of a fen peatland, Canada. *Hydrological Processes* **20**:3589-3600.
5 753
6
7 754 Winter TC. 2000. The vulnerability of wetlands to climate change: a hydrologic landscape
8 perspective. *Journal of the American Water Resources Association* **36**(2):305-311.
9 755
10
11 756 Winter TC. 2007. The role of ground water in generating streamflow in headwater areas and in
12 maintaining base flow. *Journal of the American Water Resources Association* **43**(1):15-25.
13 757
14
15
16 758
17
18
19
20
21
22
23
24
25
26
27
28
29
30
31
32
33
34
35
36
37
38
39
40
41
42
43
44
45
46
47
48
49
50
51
52
53
54
55
56
57
58
59
60

For Peer Review

759 **Table 1. Seasonal net precipitation, recharge, baseflows (for the gauging station locations**
 760 **shown in Figure 1 estimated with Champan, 1999, and simulated) and aquifer-peatland**
 761 **exchanged fluxes (estimated with Darcy and simulated) for the 2007-2010 period**

	Spring	Summer	Fall	Winter
Net precipitation (mm)	0-132* (79)**	-66-36 (-31)	102-227 (150)	133-285 (213)
Calibrated recharge for transient state simulation (mm)	40-119 (87)	0-11 (3)	31-69 (46)	0-0*** (0)
Chapman baseflow (m³/s)				
- Allen River	0.18-0.40 (0.26)	0.05-0.12 (0.09)	0.07-0.17 (0.12)	n.a.
- Outardes River	0.15-0.40 (0.27)	0.02-0.15 (0.07)	0.02-0.18 (0.09)	n.a.
- Schulman stream	0.018-0.024 (0.021)	0.002-0.004 (0.003)	0.001-0.002 (0.002)	n.a.
Simulated baseflow (m³/s)				
- Allen River	0.12-0.20 (0.16)	0.09-0.10 (0.10)	0.11-0.15 (0.13)	0.08-0.09 (0.09)
- Outardes River	0.11-0.24 (0.19)	0.06-0.07 (0.07)	0.10-0.16 (0.12)	0.05-0.06 (0.06)
- Schulman stream	0.010-0.022 (0.017)	0.007-0.008 (0.007)	0.009-0.014 (0.011)	0.006-0.007 (0.007)
Darcy aquifer-peatland flow (m³/s)	(0.0082)	(0.0076)	(0.0080)	n.a.
Simulated aquifer-peatland flow (m³/s)	0.0047-0.0090 (0.0072)	0.0034-0.0041 (0.0037)	0.0046-0.0065 (0.0053)	0.0029-0.0034 (0.0032)

762 *: minimum and maximum values

763 **: average value

764 ***: winter recharge is applied in the spring (i.e. when snow melts)

765 n.a.: data not available

766

767

768 **Table 2. Calibrated annual recharge rates for each recharge zone under current conditions**

Zone	Type of surface deposits	Calibrated recharge (mm y ⁻¹)
1	Peatland	372
2	Till over Flatrock	117
3	Till	219
4	Fractured bedrock	329
5	Shallow till over fractured bedrock	303
6	Fractured bedrock	183
7	Post-glacial littoral sediments	128
8	Compact till, silt and clay sediments	0

769

770

771 **Table 3. RCM runs considered in this study (see Mearns et al. 2012 for model acronym**
 772 **details)**

RCM	GCM	Member	Domain	Emissions scenario
CRCM4.2.3	CGCM3	5	AMNO	A2
CRCM4.2.3	CGCM3	2	AMNO	A2
CRCM4.2.3	ECHAM5	1	AMNO	A2
CRCM4.2.3	ECHAM5	2	AMNO	A2
CRCM4.2.3	Arpège UnifS2	--	AMNO	A1B
CRCM4.2.0	CGCM3	4	AMNO.	A2
HRM3	HADCM3	--	QC	A2
CRCM	CCSM	--	N. Amer.	A2
ECP2	GFDL	--	N. Amer.	A2
RCM3	CGCM3	--	N. Amer.	A2

773

774

775

1
2
3
4
5
6
7
8
9
10
11
12
13
14
15
16
17
18
19
20
21
22
23
24
25
26
27
28
29
30
31
32
33
34
35
36
37
38
39
40
41
42
43
44
45
46
47
48
49
50
51
52
53
54
55
56
57
58
59
60

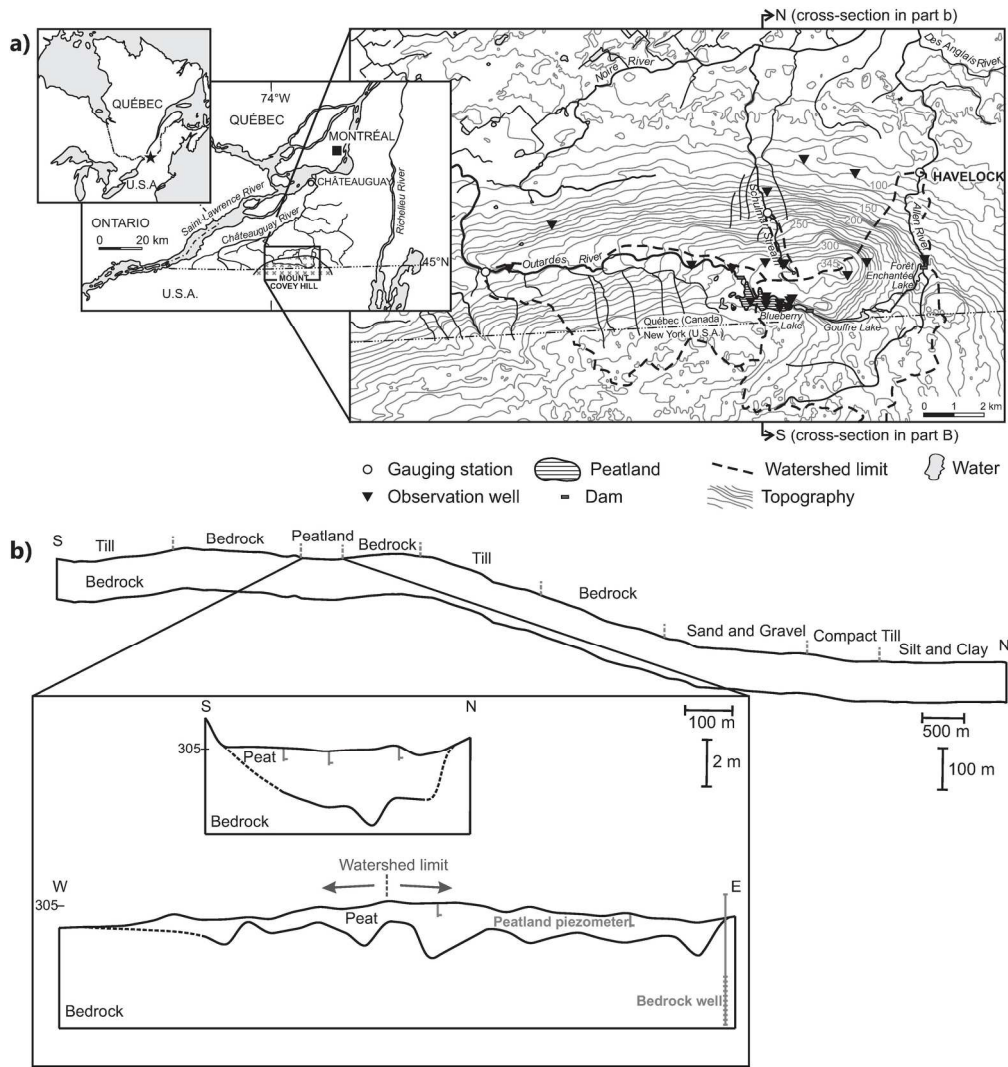
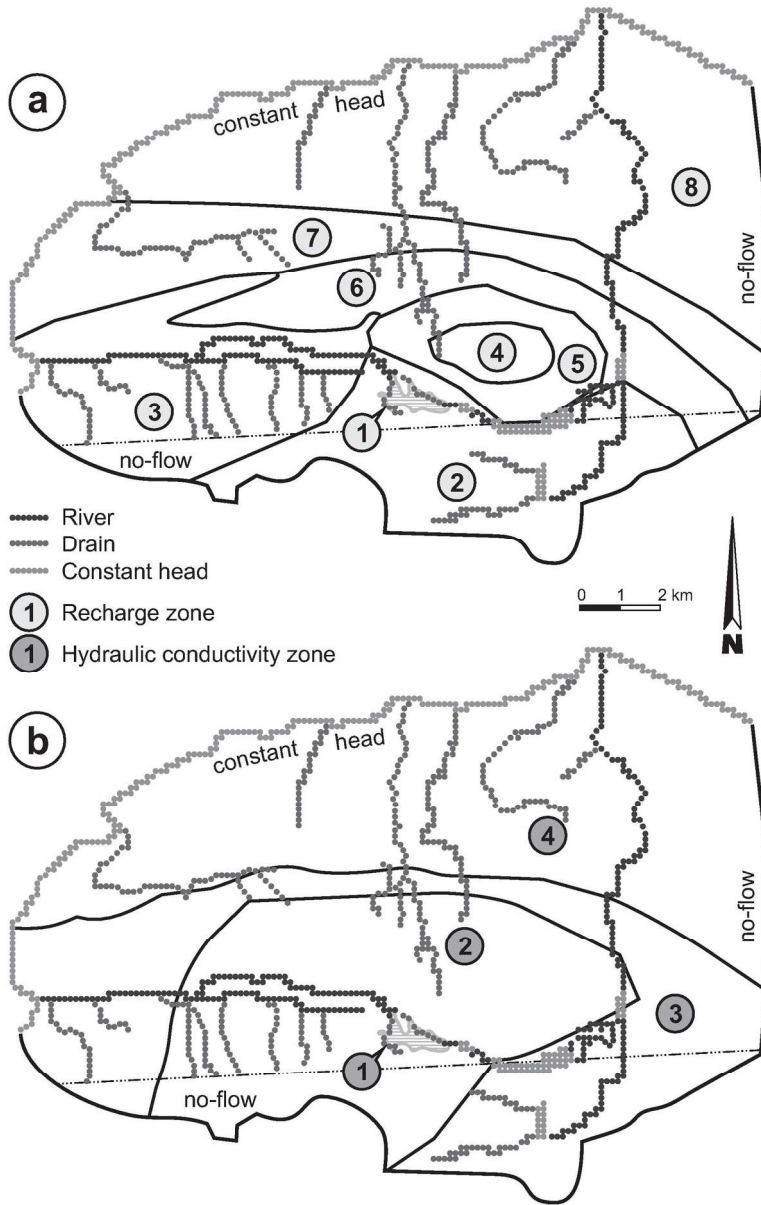
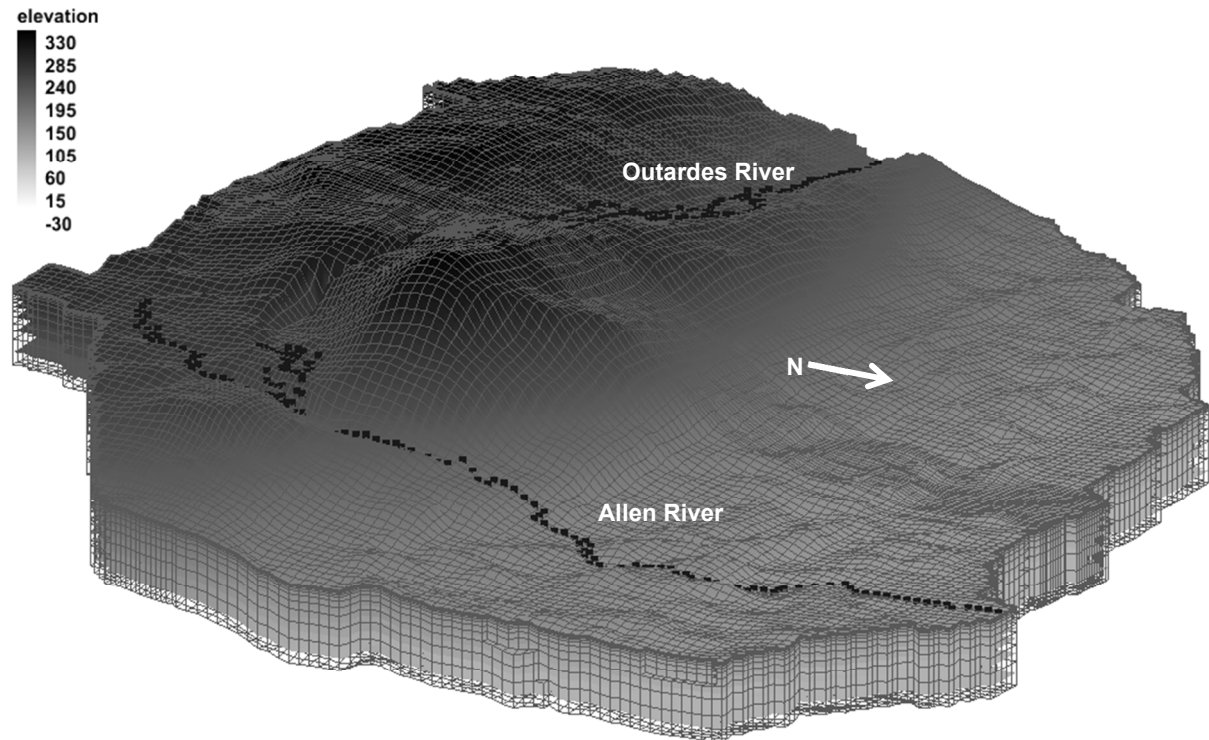


Figure 1. a) location of the Covey Hill Natural Laboratory and b) regional and peatland cross-sections. Note that SIH wells are not represented in this figure. The delineated "watershed limits" correspond to the gauging station watersheds.
188x199mm (300 x 300 DPI)

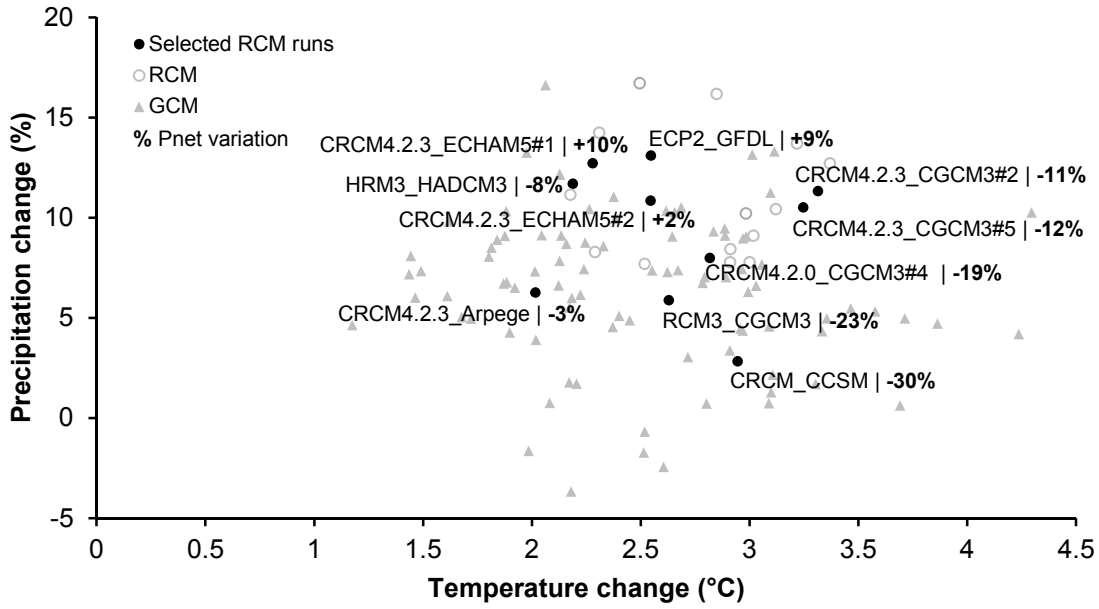


The conceptual groundwater flow model of Covey Hill: a) recharge zones and b) hydraulic conductivity zones
130x205mm (300 x 300 DPI)

1
2
3
4
5
6
7
8
9
10
11
12
13
14
15
16
17
18
19
20
21
22
23
24
25
26
27
28
29
30
31
32
33
34
35
36
37
38
39
40
41
42
43
44
45
46
47
48
49
50
51
52
53
54
55
56
57
58
59
60

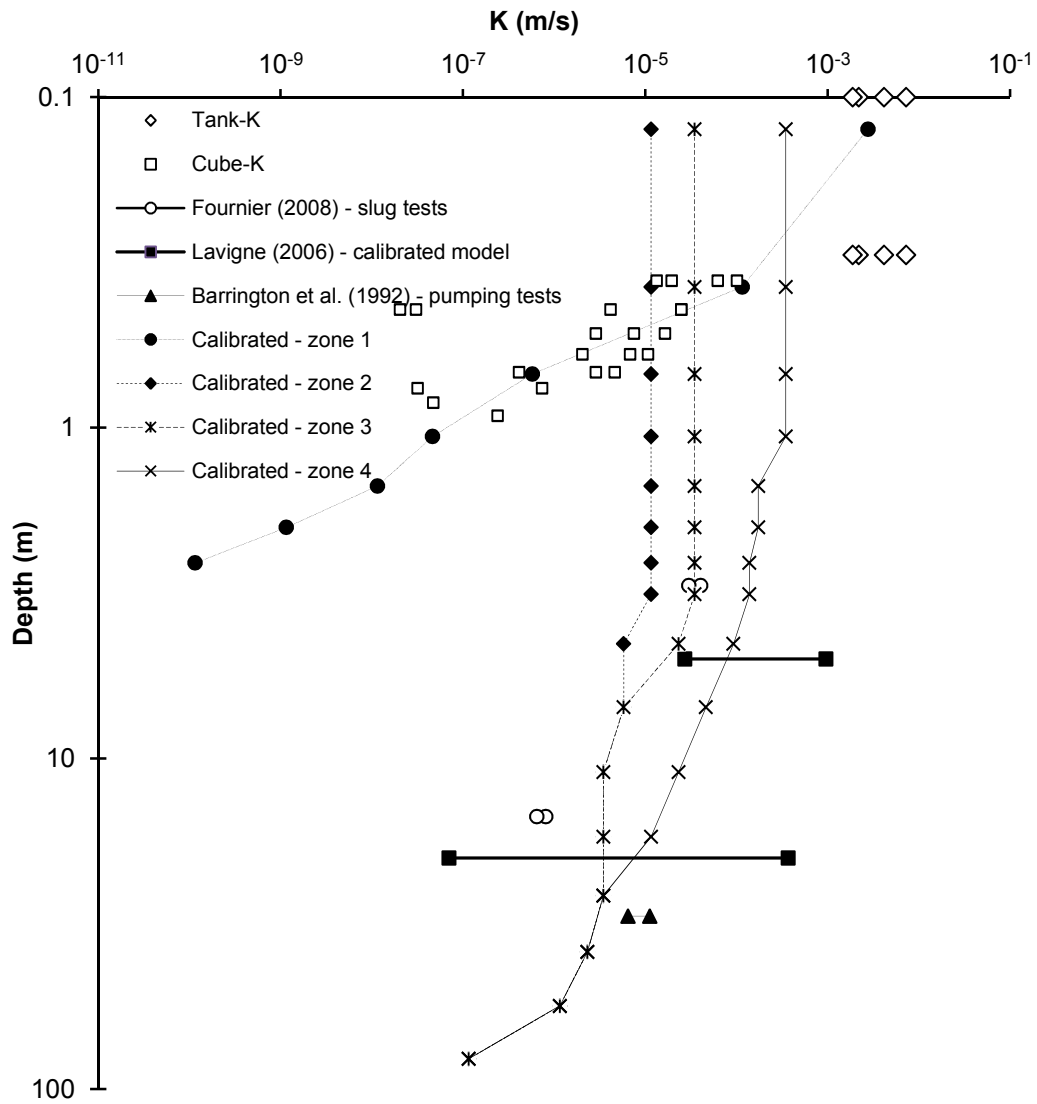


Peer Review

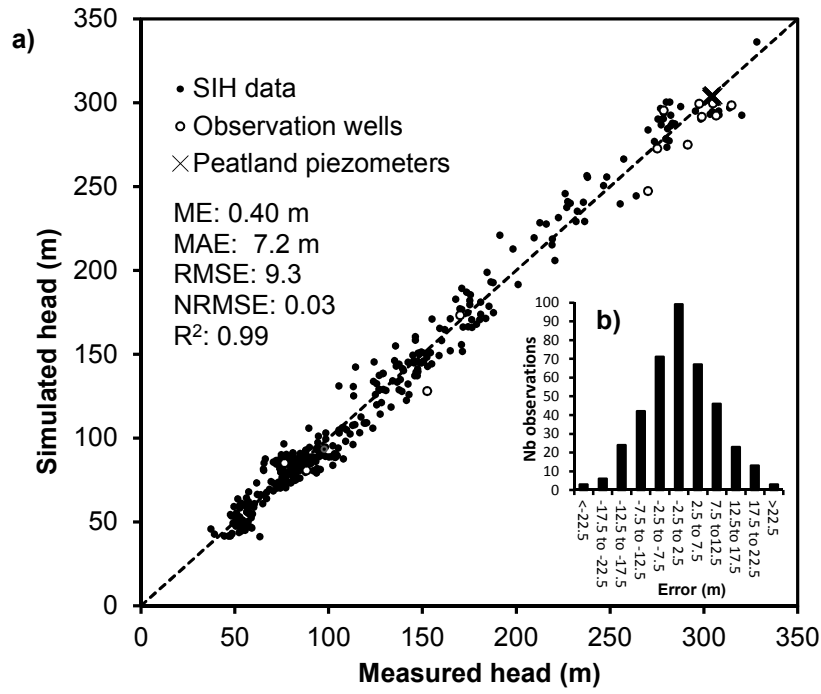


Peer Review

1
2
3
4
5
6
7
8
9
10
11
12
13
14
15
16
17
18
19
20
21
22
23
24
25
26
27
28
29
30
31
32
33
34
35
36
37
38
39
40
41
42
43
44
45
46
47
48
49
50
51
52
53
54
55
56
57
58
59
60

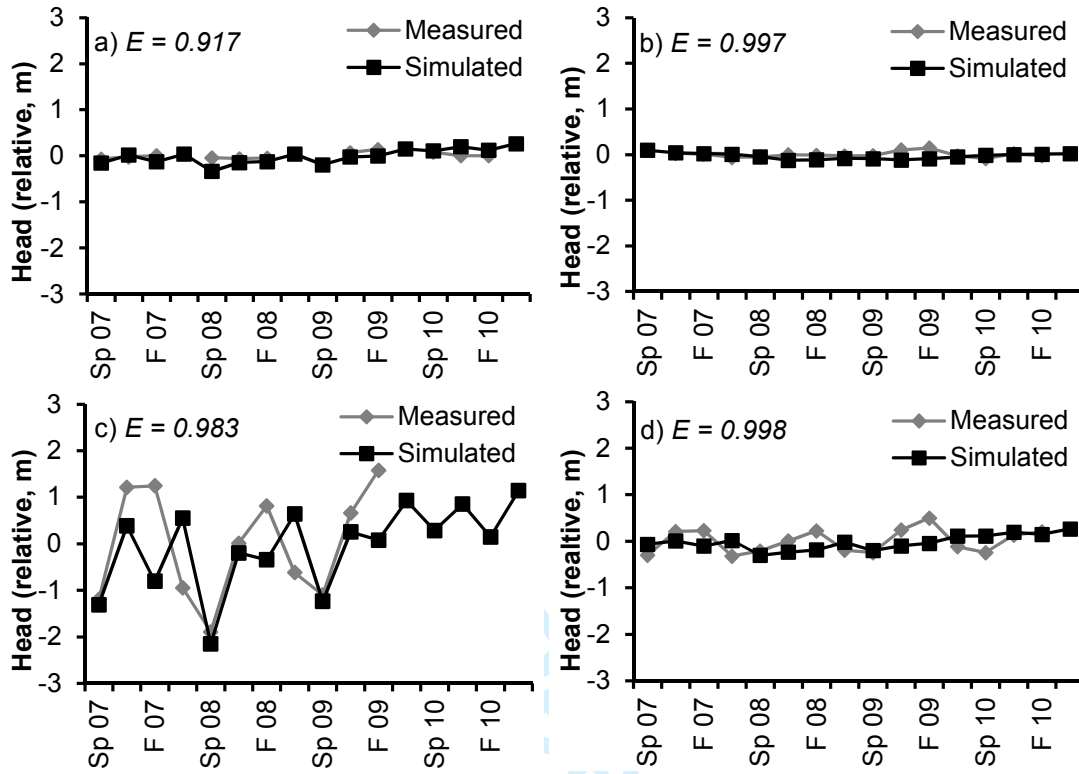


1
2
3
4
5
6
7
8
9
10
11
12
13
14
15
16
17
18
19
20
21
22
23
24
25
26
27
28
29
30
31
32
33
34
35
36
37
38
39
40
41
42
43
44
45
46
47
48
49
50
51
52
53
54
55
56
57
58
59
60



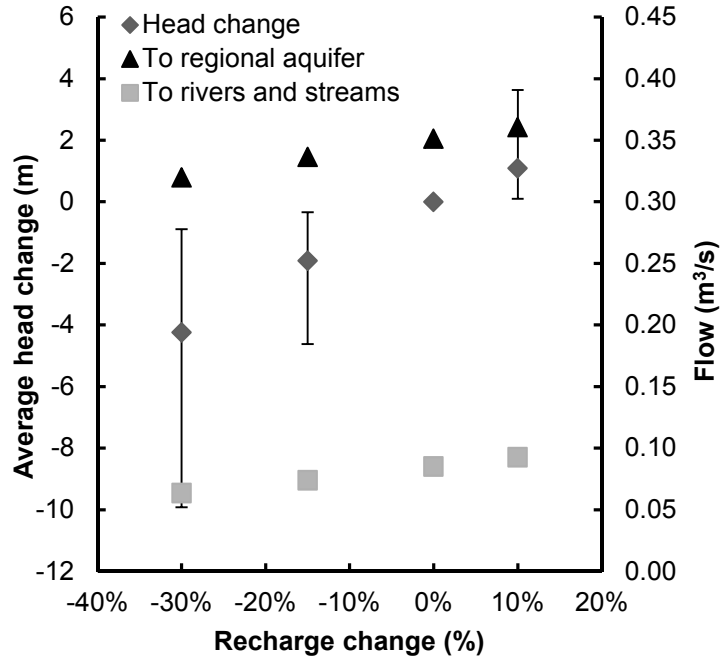
Peer Review

1
2
3
4
5
6
7
8
9
10
11
12
13
14
15
16
17
18
19
20
21
22
23
24
25
26
27
28
29
30
31
32
33
34
35
36
37
38
39
40
41
42
43
44
45
46
47
48
49
50
51
52
53
54
55
56
57
58
59
60



Review

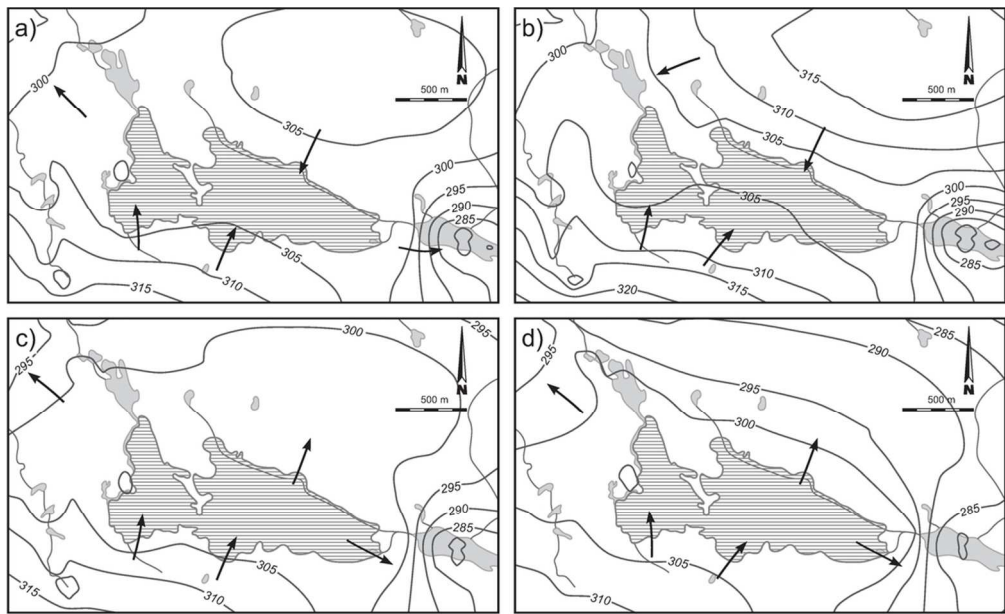
1
2
3
4
5
6
7
8
9
10
11
12
13
14
15
16
17
18
19
20
21
22
23
24
25
26
27
28
29
30
31
32
33
34
35
36
37
38
39
40
41
42
43
44
45
46
47
48
49
50
51
52
53
54
55
56
57
58
59
60



Peer Review

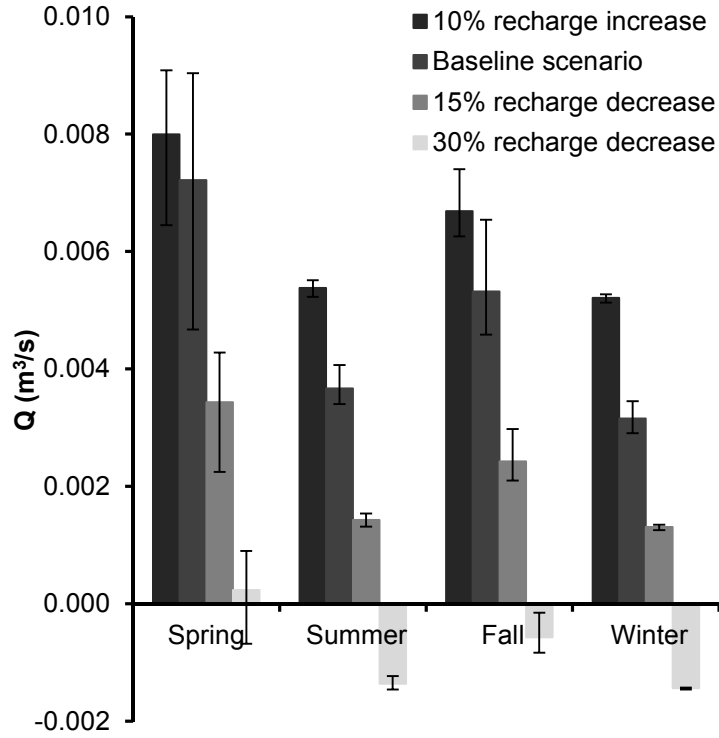
1
2
3
4
5
6
7
8
9
10
11
12
13
14
15
16
17
18
19
20
21
22
23
24
25
26
27
28
29
30
31
32
33
34
35
36
37
38
39
40
41
42
43
44
45
46
47
48
49
50
51
52
53
54
55
56
57
58
59
60

1
2
3
4
5
6
7
8
9
10
11
12
13
14
15
16
17
18
19
20
21
22
23
24
25
26
27
28
29
30
31
32
33
34
35
36
37
38
39
40
41
42
43
44
45
46
47
48
49
50
51
52
53
54
55
56
57
58
59
60



Simulated flow directions in the peatland contribution area a) for spring 2010, and for the recharge scenarios b) 10% increase, c) 15% decrease and d) 30% decrease
103x62mm (300 x 300 DPI)

Review



Peer Review

1
2
3
4
5
6
7
8
9
10
11
12
13
14
15
16
17
18
19
20
21
22
23
24
25
26
27
28
29
30
31
32
33
34
35
36
37
38
39
40
41
42
43
44
45
46
47
48
49
50
51
52
53
54
55
56
57
58
59
60